Science of the Total Environment 967 (2025) 178794

Contents lists available at ScienceDirect

Science of the Total Environment

journal homepage: www.elsevier.com/locate/scitotenv

Batch and semi-batch anaerobic digestion of poly (3-hydroxybutyrate-*co*-3-hydroxyhexanoate) (PHBH) bioplastic: New kinetic, structural, microbiological and digestate phytotoxicity insights

Mohamed Shafana Farveen [a,b], Raul Muñoz [a,c], Rajnish Narayanan [b], Octavio García-Depraect [a,c,*]

[a] Institute of Sustainable Processes, Dr. Mergelina s/n, 47011 Valladolid, Spain
[b] Department of Genetic Engineering, College of Engineering & Technology (CET), SRM Institute of Science and Technology, Kattankulathur, Chennai, Tamil Nadu, India
[c] Department of Chemical Engineering and Environmental Technology, School of Industrial Engineering, University of Valladolid, Dr. Mergelina, s/n, 47011 Valladolid, Spain

HIGHLIGHTS

- Semi-batch anaerobic digestion achieved 562 NmL CH_4/g VSadded and 281 NmLCH_4/L-d.
- Carbon mass balance showed 96.09 % recovery, with 84.3 % converted to biogas.
- Surface erosion was determined as the primary biodegradation mechanism.
- The dominance of *Methanosaeta* suggests acetoclastic methanogenesis.
- Digestate exhibited phytotoxicity, suggesting the presence of inhibitory compounds.

GRAPHICAL ABSTRACT

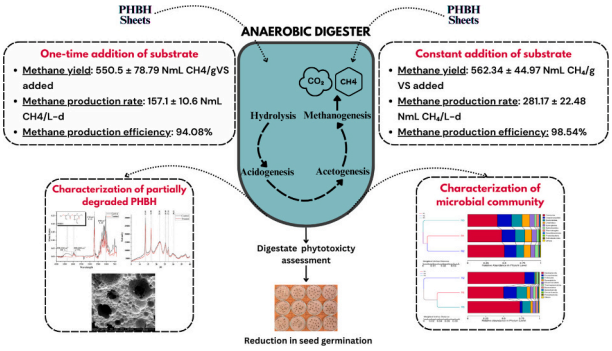

ARTICLE INFO

Editor: Yifeng Zhang

Keywords:
Anaerobic digestion
Biodegradation
Bioplastic
Digestate phytotoxicity
Microbial analysis

ABSTRACT

This study investigated the bioconversion of poly(3-hydroxybutyrate-*co*-3-hydroxyhexanoate) (PHBH) in batch and semi-batch anaerobic digestion systems, focusing not only on methane production and microbial community dynamics, but also on the structural changes that occur during degradation and the potential use of the resulting digestate as a soil enhancer. Both systems operated under mesophilic conditions (37 ± 2 °C) and stable pH (7.9 ± 0.2). The batch system achieved a methane yield of 550.5 ± 78.79 NmL CH_4/g VS added over 50 days, with a typical sigmoidal methane production pattern. A carbon mass balance analysis indicated a 96.09 % recovery, with 47.62 % of the carbon converted to methane. SEM, FTIR and XRD analyses of the partially degraded material showed that the anaerobic biodegradation of PHBH was characterized by surface erosion and weight loss, with minimal changes in crystallinity. Conversely, the adaptation of the microbial community to 93 days of continuous PHBH feeding allowed the achievement of a stable methane yield of 562.34 ± 44.97 NmL CH_4/g VS added, along with a corresponding volumetric methane production rate of 281.17 ± 22.48 NmL CH_4/L-d.

* Corresponding author at: Department of Chemical Engineering and Environmental Technology, School of Industrial Engineering, University of Valladolid, Dr. Mergelina, s/n, 47011 Valladolid, Spain.
E-mail address: octavio.garcia@uva.es (O. García-Depraect).

https://doi.org/10.1016/j.scitotenv.2025.178794
Received 24 September 2024; Received in revised form 23 January 2025; Accepted 6 February 2025
Available online 12 February 2025

Microbial community analysis, at pseudo-steady state, revealed the dominance of *Methanosaeta*, *Anaerolineaceae*, and *Thermovirga* in driving the anaerobic digestion of PHBH via acetoclastic methanogenesis. Despite high methane production efficiency, digestate toxicity tests using perennial ryegrass indicated phytotoxic effects on seed germination, highlighting the need for further investigation to characterize inhibitory compounds and develop mitigation strategies.

1. Introduction

Plastic pollution remains a critical global issue with significant consequences for environmental ecosystems and human health. Studies have shown that the extensive use of plastics, particularly single-use items like grocery bags and face masks, poses challenges for waste management systems (Ahamed et al., 2021; Selvaranjan et al., 2021). Due to the increasing demand for plastic products, it is essential to explore strategies for implementing circular economy practices and improving plastic waste management to mitigate their environmental impact (Ganguly and Chakraborty, 2024). In this context, the use of bioplastics has emerged as a sustainable alternative to conventional plastics, offering advantages such as biodegradability, reduced reliance on fossil fuels, and lower environmental impact. The bioplastics market can be strengthened by developing efficient waste management systems that ensure proper collection, recycling, and end-of-life treatment, maximizing their environmental and economic benefits (Atiwesh et al., 2021). Among various bioplastics, polyhydroxybutyrate-*co*-3-hydroxyhexanoate (PHBH) has gained attention for its biodegradability and mechanical properties, making it suitable for applications in packaging, agriculture, and medical devices (Eraslan et al., 2022).

Anaerobic digestion (AD) represents a promising method for managing bioplastic waste while simultaneously producing bioenergy (in the form of biogas) and digestate which has the potential to be used as fertilizer (Cucina et al., 2021; Slepetiene et al., 2020). Several studies have investigated the effectiveness of AD in the degradation of different bioplastics under various conditions (Cazaudehore et al., 2022; Cazaudehore et al., 2023a). To date, research on the anaerobic degradation of PHBH has been limited exclusively to batch test studies (García-Depraect et al., 2024). While batch systems provide initial insights into degradation rates and biogas yield, it is worthy to note that the batch mode present limitations in accurately simulating full-scale continuous AD systems (Dolci et al., 2022). Furthermore, batch tests fail to capture key aspects of anaerobic degradation, such as long-term process stability, methane productivity, organic loading rates, and the impacts of continuous feeding on factors such as nutrient depletion, microbial acclimatization, and the accumulation of toxicants (Koch et al., 2020). Recently, microbial acclimatization in semi-continuous digesters has been reported as a key factor in promoting the enrichment of microorganisms capable of degrading bioplastics, such as starch-based bioplastics (SBS) and polylactic acid (PLA) (Clagnan et al., 2023). In this context, bioplastics have been shown to shape the microbial community structure during AD (Bandini et al., 2022). However, how PHBH may influence the microbiome driving the AD process remains unknown. In this context, a more in-depth investigation into the continuous AD of PHBH, as well as the specific microbiome composition driving the process, is essential to advance understanding and optimize process performance.

The present study aims at investigating the methanization of PHBH in both batch and semi-batch AD systems. Additionally, the structural transformation of PHBH during degradation was analyzed using analytical techniques, i.e., X-ray diffraction (XRD), Scanning electron microscopy (SEM), and Fourier transform infrared spectroscopy - attenuated total reflectance (FTIR-ATR). In addition, the microbial community structure enriched during the continuous feeding of PHBH was characterized. Finally, this study evaluated the digestate derived from the semi-batch PHBH AD through phytotoxicity testing, using perennial ryegrass as a model seed species. The novel contributions of this study are as follows: i) it provides the first comparative analysis of PHBH methanization under batch and semi-batch operational systems, including a taxonomic analysis of the microbiota involved; ii) it investigates structural changes in PHBH during the degradation process; and iii) it evaluates the phytotoxic potential of PHBH-derived digestate as a preliminary step toward assessing its viability as a safe and efficient alternative soil amendment.

2. Materials and methods

2.1. Plastic material and inoculum

In this study, PHBH sheets with a thickness of 0.9 mm were used as the substrate. The PHBH, represented by the chemical formula $[(C_4H_6O_2)_m(C_6H_{10}O_2)_n]$, has the copolymer composition of <10 mol% 3-hydroxyhexanoate (3HH), with the remainder consisting of 3-hydroxybutyrate (3HB). Elemental analysis using Energy-Dispersive X-ray Spectroscopy (EDAX) confirmed that the PHBH sheet comprised 68.51 % carbon and 31.49 % oxygen (see Supplementary material). Anaerobic sewage sludge, sourced from the domestic wastewater treatment plant in Valladolid, Spain, was employed as the inoculum. A comprehensive analysis of the physical and chemical properties of the sludge was carried out prior to its use in the study. Total solids (TS) and volatile solids (VS) were found to be 19.26 g/kg and 11.85 g/kg, respectively. Total dissolved organic carbon was 117.65 mg/L, dissolved inorganic carbon was 797.06 mg/L and ammonia nitrogen was 941.73 mg/L. The pH was measured to be 7.97 ± 0.2.

2.2. Batch mode

Biochemical methane potential (BMP) tests were conducted to assess the anaerobic biodegradability of PHBH. The methanogenic sludge was preincubated for 7 days at 37 ± 2 °C to minimise the background methane production. A working volume of 0.5 L anaerobic sewage sludge in 2.1 L glass digesters under mesophilic conditions (37 ± 2 °C) was used for the experiment. In the experimental setup, nine digesters were operated in total, consisting of three blank controls containing only inoculum and six dedicated to the degradation of PHBH. The blank controls were used to measure baseline methane production from the inoculum, allowing for normalization to account for any residual methane activity originating from the inoculum. Additionally, three PHBH digesters in the BMP test were randomly terminated during the exponential methane production phase to collect partially degraded bioplastic samples for investigating the structural changes occurring during methanization. Approximately three PHBH sheets, each measuring 3 × 3 cm, were added to each BMP bottle, corresponding to a total of 2.96 g based on the VS composition of the sludge, maintaining a food-to-microorganisms (F/M) ratio of 0.5 (VS basis) consistent with previous studies (Shrestha et al., 2020). Sodium bicarbonate ($NaHCO_3$) at the concentration of 5 g/L was added as a buffering agent to avoid acidification of the system. Final pH remained at 7.9 ± 0.2 for all conditions tested. The anaerobic condition was maintained by sealing the digesters with butyl rubber septa and aluminium caps, which were then purged with helium gas (Abello Linde, Barcelona, Spain) at 0.5 bar for 5 min. Digesters were incubated at 37 ± 2 °C in a Wheaton roller apparatus (Scientific Products, USA) at 4.5 rpm. Biogas production was monitored every alternate day, and cumulative methane production was calculated by the standard manometric method (García-Depraect et al.,

2023; Himanshu et al., 2017) along with the determination of biogas composition by GC-TCD. The experiment concluded once the daily methane production dropped below 1 % of the total cumulative methane production for three consecutive days (Angelidaki et al., 2009; García-Depraect et al., 2022b). On completion of the incubation period, the samples were analyzed for weight loss, pH, dissolved inorganic carbon, and total organic carbon. Ultimately, the fate of the carbon introduced into the system was determined by performing a carbon mass balance analysis. The total carbon recovery was calculated as a percentage of the initial carbon input by quantifying the carbon distributed among intermediates and end-products. This included the carbon content of VFAs, organic and inorganic carbon in the liquid effluent, gaseous carbon in the forms of carbon dioxide and methane (García-Depraect et al., 2022a). The carbon content associated with the residual material was also included in the analysis. The amount of residual PHBH material was measured by sieving it through a 1 mm mesh and rinsing with tap water. It was also assumed that 10 % of the total initial carbon was incorporated into the biomass (Chernicharo, 2007).

2.3. Semi-batch mode

An anaerobic digester with a total volume of 3.1 L (2 L working volume) was operated for 112 days, using the same methanogenic inoculum as in the batch tests, to establish a stable microbial community responsible for methane production from PHBH. The pH remained at 7.9 ± 0.2, while the temperature and mixing rate were kept constant at 37 °C and 200 rpm, respectively, throughout the operation. The digester was initially filled with 2 L of inoculum and 1 g of PHBH. To provide buffering capacity and to prevent exhaustion of micronutrients in the system, the following components were also added at the start of the experiment: KH_2PO_4 (0.27 g/L), $Na_2HPO_4{\cdot}12H_2O$ (0.44 g/L), NH_4Cl (0.53 g/L), $CaCl_2{\cdot}2H_2O$ (0.075 g/L), $MgCl_2{\cdot}6H_2O$ (0.1 g/L), $FeCl_2{\cdot}4H_2O$ (0.027 g/L), $Na_2S{\cdot}9H_2O$ (0.1 g/L), and $NaHCO_3$ (5 g/L). The digester was operated in batch mode for the first 5 days of operation. From day 6 to day 99, 1 g of PHBH was fed into the digester every day to achieve an organic loading rate (OLR) of 0.5 g VS/L-d. To add the plastic, the stirring was temporarily stopped for 1 min, during which square pieces of plastic, approximately 0.5 cm in size, were added. This involved opening one of the ports on the digester lid for 10–15 s to introduce the plastic. After the plastic was added, the port was promptly sealed with a butyl rubber stopper, and the stirrer was then reactivated. On day 99, the continuous feeding of PHBH was halted to assess the methane production from residual materials still present in the digester. No liquid was added or removed from the digester throughout the entire experiment, except for the periodic sampling of 5 mL for VFAs, pH and microbiological analysis, with the total volume collected remaining below 5 % of the reactor's total volume. It is worth mentioning that the working volume of the reactor remained relatively constant throughout the experiment, despite the continuous addition of PHBH, likely due to the effective polymer degradation and conversion of its by-products into biogas. Routine analysis of biogas production and composition was performed using a liquid displacement gasometer and GC-TCD, respectively. Weekly assessments of pH and VFA were also conducted following the onset of exponential methane production to ensure optimal reactor performance, avoiding excessive acidification.

2.4. Analytical techniques

Standard methods were employed for the determination of solids (American Public Health Association, 1995). Headspace overpressure in the BMP bottles was measured using an IFM electronic PN7097 pressure transducer, while the gas composition was measured using gas chromatography equipped with a thermal conductivity detector (GC-TCD), Varian CP-3800, USA. Gas samples from the headspace were injected into the GC-TCD using a 100 μL gas-tight syringe. The GC-TCD setup was equipped to detect a range of gases, including carbon dioxide, methane, hydrogen sulphur, nitrogen, and hydrogen; however, this study prioritized methane and carbon dioxide measurements as key indicators of the AD performance. Separation of CO_2 and CH_4 was achieved using CP-Molsieve 5A and CP-PoraBOND Q capillary columns. Helium served as the carrier gas. Cumulative methane yield was calculated according to Angelidaki et al. (2009). Methane production efficiency was calculated as the percentage of experimental methane yield relative to the theoretical methane yield (Raposo et al., 2011). The total organic carbon (TOC), inorganic carbon (IC), and total nitrogen (TN) concentrations were analyzed using a Shimadzu TOC-VCSH analyzer equipped with a TNM-1 chemiluminescence module. VFA profiles were established using a gas chromatograph (Agilent 7820A) equipped with a flame ionization detector and a TEKNOKROMA NF29370-F packed column. The GC oven temperature was programmed for a gradient increase from 135 °C to 180 °C, with a final hold at 180 °C. Nitrogen served as the carrier gas, while hydrogen and air were utilized for the flame ionization detector. Prior to all analyses, the samples were prepared by centrifugation at 10,000 rpm for 10 min, followed by filtration through a 0.2 μm filter, and then acidification using concentrated sulfuric acid.

2.5. Characterization of the bioplastic

To investigate the structural changes that occur during the anaerobic degradation of PHBH, partially degraded plastic fragments were collected from the BMP tests, specifically from three batch digesters that were randomly sacrificed on day 25, corresponding to the exponential phase of methane production. These fragments were rinsed with water, air-dried at 37 °C overnight, and then weighed. Subsequently, instrumental analyses were performed to assess structural changes. Crystallinity assessment was performed using XRD analysis on a Bruker Discover D8 instrument. The XRD was operated in wide-angle mode with 40 kV and 30 mA, employing an average wavelength of $\lambda = 1.54$ Å. Diffractograms were recorded from 5° to 50° at 2θ, with a 0.02° angular increment at room temperature (Farrag et al., 2022). OriginPRO 2022b software was utilized to process the diffraction patterns and determine crystallinity levels. Morphological changes were investigated using SEM analysis with a QUANTA 200 FEG instrument operating in high vacuum mode. Prior to imaging, samples were sputter-coated with gold for 60 s to enhance conductivity and image quality. Elemental mapping was conducted using the EDAX Genesis system. Chemical structure modifications were analyzed via FTIR-ATR analysis using a Thermo Scientific Nicolet iS50 spectrometer Spectra were acquired in the range of 4000 to 400 cm^{-1} (Yan et al., 2021). An untreated PHBH sample served as a control for all analyses, allowing for a comparative assessment of the biodegradation-induced changes.

2.6. Microbial analysis

Triplicate digestate samples (R1, R2, R3) were collected at three different time points (Day 42, day 63, day 92) during the pseudo-steady state of the semi-batch reactor to gain insights into the dominant microbial communities driving the AD of PHBH. The total genomic DNA extraction was performed using FastDNA™ SPIN Kit for Soil according to the manufacturer's instructions and quantified using Qubit™ dsDNA HS assay kits. The obtained DNA samples were sequenced, targeting the V4-V5 region of 16S rRNA by Novogene, Europe. The primer set 515F-944R was used to PCR amplify the hypervariable region V4-V5 to study the bacterial community. Meanwhile, the V4 region was targeted using the 519F-806R primer set to study the archaeal community. Phusion® High -Fidelity PCR Master Mix (New England Biolabs) was used to perform all PCR amplifications. Following the purification, quantification, and library preparation of the PCR-amplified target regions, 250 bp paired-end reads were generated by sequencing on the Illumina NovaSeq platform. The raw sequences obtained were trimmed using Cutadapt (v3.3) with default parameters to remove the adaptors introduced during the library preparation process. Subsequently, the

trimmed reads were merged using FLASH (v1.2.11) (Magoč and Salzberg, 2011), which merges the overlapping reads of opposite ends of the same DNA fragment. Fastp (v0.23.1) was used for quality filtering, resulting in high-quality reads (Q20). Chimera sequences detection was performed by comparing the quality-filtered sequences with the reference database and was removed using the vsearch package (v2.16.0) (Edgar et al., 2011). To identify unique amplicon sequence variants (ASVs), denoising was performed using DADA2, implemented within the QIIME 2 software package. The high-quality reads were used for species annotation against the reference database (Silva database v138.1 (16S) and the Micro_NT database) (Quast et al., 2013). The phylogenetic relationship of the annotated sequences was built using the MUSCLE software (v3.3.31) (Edgar, 2004). Subsequent alpha, beta diversity analyses and data visualization were performed using R software (Version 4.0.3). The raw sequence data has been deposited in the NCBI GenBank's Sequence Read Archive (SRA) under BioProject accession number PRJNA1162757.

2.7. Digestate phytotoxicity test

Seed germination assays with perennial ryegrass (*Lolium perenne*) were used to assess digestate toxicity and its potential as a fertilizer, following established methods (Xu et al., 2021; Zhang et al., 2015). The assay involved exposing seeds to various concentrations of soluble elements in digestate to determine potential phytotoxic effects. The digestate was collected on day 99 from the semi-batch anaerobic digester. The digestate was centrifuged at 11,000 rpm for 5 min and filtered using 47 mm filter paper to remove solid particles, including residual bioplastic, ensuring a uniform liquid phase for a more accurate analysis. For the phytotoxicity assessment, final concentrations of 10 %, 20 %, and 40 % digestate were prepared by diluting the filtrate with sterile distilled water. Healthy grass seeds, carefully selected for their intact embryos, were only used in this test. Distilled water served as the positive control. All dilutions and the control were assessed in triplicate, with each replicate consisting of fifteen seeds in a 90 mm diameter Petri dish lined with filter paper, moistened with 2 mL of each digestate dilution. To maintain moisture and prevent seed desiccation, 1 mL of the respective digestate concentration was added after 48 h. The seeds were then incubated in the dark at 25 °C for 96 h. The seed germination index assessing the combined effects of seed germination and the root development, was monitored as an indicator of phytotoxicity. This index is mathematically expressed as the product of the relative seed germination (the germination rate of treated seeds compared to control seeds) and the relative root length (the root length of treated seeds compared to control seeds), with the result expressed as a percentage (Martínez-Cruz and Rojas-Valencia, 2024).

2.8. Data analysis

All experimental data were obtained from triplicate measurements, with standard deviations calculated to assess data variability. The volumes of biogas reported were normalized to standard temperature and pressure conditions (0 °C and 1 atm). The kinetics of methane production in the batch tests were evaluated using the modified Gompertz model (Eq. 1), where H represents the total cumulative methane production (NmL), λ denotes the lag phase duration (days), t is the culture duration (days), P signifies the maximum cumulative methane production (NmL), Rm refers to the maximum specific methane production rate (NmL CH_4/g VS-d), and e is the Euler's number, approximately equal to 2.71828.

$$H(t) = P\,exp\left\{ -exp\left[\frac{Rm \bullet e}{P}(\lambda - t) + 1\right]\right\} \quad (1)$$

3. Results and discussion

3.1. Biogas production

Notable differences in the dynamics of methane production were observed between the batch and semi-batch operation systems, indicating distinct behaviours in the biodegradation kinetics of PHBH. In batch-mode operation, the methane production exhibited a typical sigmoidal pattern, characterized by an initial lag phase lasting approximately 12 days (Fig. 1). As the inoculum used was not adapted to PHBH (as the only carbon source), the observed lag phase likely reflects the time required for microbial communities to acclimate and initiate the hydrolysis of the polymer (Bandini et al., 2022; Ryan et al., 2017). Following this acclimation period, a pronounced exponential increase in methane production was observed over the subsequent 28 days, indicating active microbial involvement in substrate metabolization. Around day 40, the batch-mode system entered a stationary phase (Fig. 1A). This reduction in methane production suggested the depletion of methane precursors, indicating the end of the batch process. The cumulative methane yield was calculated to be 550.5 ± 78.79 NmL CH_4/g VS added (the calculated methane yield for the digesters sacrificed for PHBH characterization is provided in the supplementary file). The biodegradation kinetics of PHBH in the batch system were analyzed using the modified Gompertz model, which provided a strong fit to the experimental data ($R^2 = 0.9962 \pm 0.0021$; Fig. 1). The model estimated a maximum methane potential (P) of 601.4 ± 87.2 NmL CH_4/g VS added. In addition, the maximum daily methane production rate was estimated to be 157.1 ± 10.6 NmL CH_4/L-d (Fig. 1B). Throughout the BMP test, VFA levels remained low, in the range of a few mg/L, with acetate showing a transient increase from 2.75 mg/L to 12.76 mg/L during the exponential methane production phase before decreasing to 9.03 mg/L by the end of the experiment, Other VFAs, such as propionic acid and butyric acid, remained below 2 mg/L (see Supplementary material).

Additionally, a carbon mass balance analysis was conducted to elucidate the fate of carbon during BMP tests (Table 1). The total carbon recovery was 96.09 % consistent with accepted ranges for experimental studies (García-Depraect et al., 2022a). A significant portion, 47.62 %, was converted to methane, while 36.68 % was recovered as gaseous CO_2, resulting in a combined 84.3 % carbon recovery in biogas. Furthermore, 1.07 % and 0.63 % of the carbon were recovered as dissolved inorganic carbon and total organic carbon in the liquid phase, respectively, with a minimal contribution from VFAs (0.09 %) indicating near-complete conversion of intermediates and a well-balanced AD process (Cazaudehore et al., 2023b). It should be noted that the carbon fate analysis considered that 10 % of the carbon present in the substrate was converted into microbial biomass (Chernicharo, 2007; García-Depraect et al., 2022a), which could explain the unaccounted carbon fraction (3.91 %). Finally, the measurements of residual material obtained at the end of the batch test showed that only a negligible amount (0.0001 %) remained as undegraded PHBH.

In contrast, the semi-batch system displayed a distinct methane production behaviour, characterized by an initial lag phase (days 6–15), followed by a sharp but temporary increase in methane production (days 16–38), and a subsequent transition to steady-state methane production (day 39–99) (Fig. 2A). The criterion used to define steady-state methane production was a 15 % variation in recorded daily methane yields over a three-week period. Under pseudo-steady conditions, the average methane productivity achieved was 281.17 ± 22.48 NmL CH_4/L-d, while the methane content in the produced biogas was approximately 58 % (*v/v*) (Fig. 2B). During the lag phase, microbial communities undergo acclimatization, synthesizing and releasing extracellular enzymes essential for hydrolysis of PHBH (Zhu et al., 2023). The accumulation of substrate due to the continuous supply of PHBH, combined with the temporary inability of the microbiota to hydrolyze and further metabolize the PHBH material, probably explains the lag phase observed. The

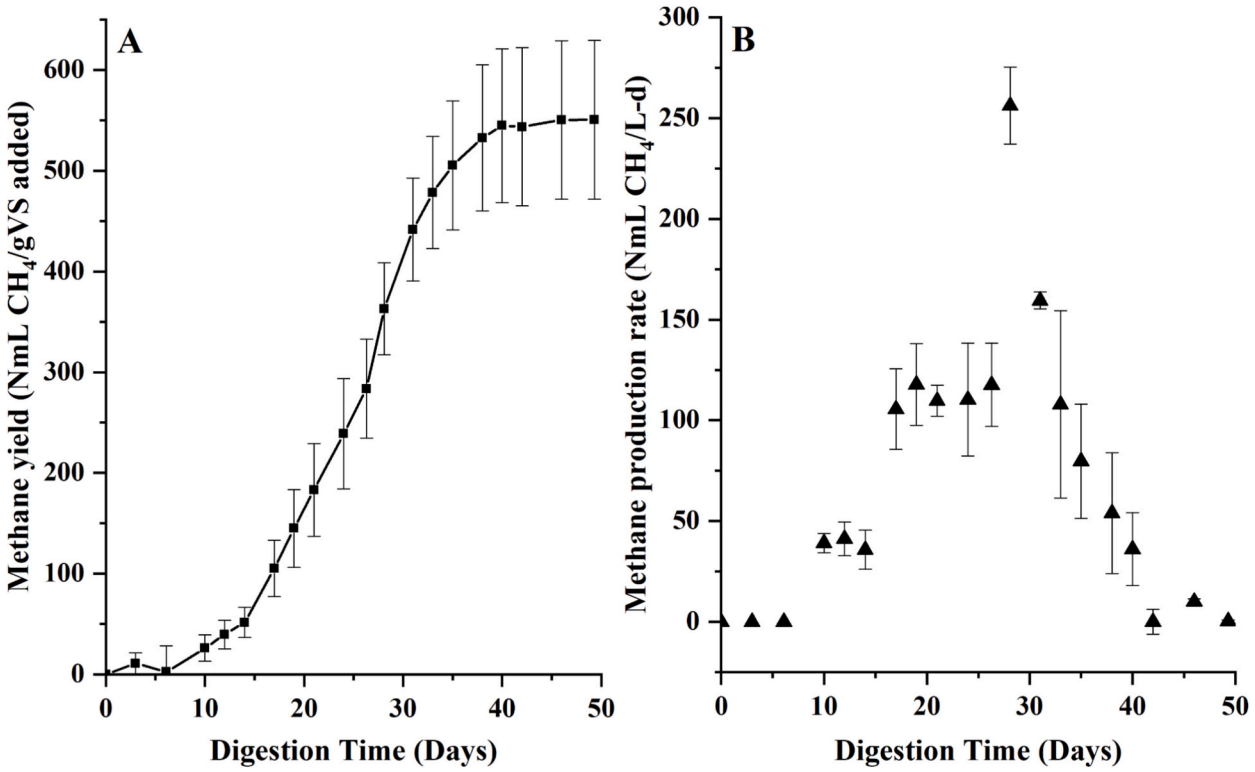

Fig. 1. Time course behaviour of (A) cumulative methane yield and (B) methane production rate during the batch anaerobic digestion of PHBH.

Table 1
Carbon fate during the batch anaerobic digestion of PHBH.

Fate of carbon	Carbon (%)
DIC	1.07
DOC	0.63
CO_2 gas	36.68
CH_4	47.62
VFAs	0.09
Microbial growth	~10 %
Residual PHBH	0.0001
***Total recovery**	**96.09**

*Carbon mass balance was assessed by comparing pre- and post-digestion carbon levels, assuming that biodegraded PHBH carbon was diverted to methane (CH_4), carbon dioxide gas (CO_2 gas), dissolved organic (DOC) and inorganic (DIC) carbon and new biomass (García-Depraect et al., 2022a). It was assumed that 10 % of the total initial carbon was incorporated into biomass (Chernicharo, 2007).

temporary increase in methane production (peak at 1275.91 NmL CH_4/g VS added with an associated methane productivity of 639.30 NmL CH_4/L-d) could be attributed to the completion of the acclimation period. Acclimated microbiota began to produce and metabolize methane precursors such as acetate, which showed a significant increase from 2.75 mg/L to 2959.51 mg/L at the peak of methane production (Fig. 2A and C). When the process reached a pseudo-steady state, acetic acid levels averaged 29.76 mg/L, while other VFAs, including propionic and butyric acids, dropped below the detection limit (Fig. 2C). During the subsequent pseudo-stable phase, an average methane yield of 562.34 ± 44.97 NmL CH_4/g VS added was recorded for over 60 days. The recorded methane output closely aligns with the theoretical yield of approximately 585.62 NmL CH_4/g VS from PHBH, as calculated by (Reischwitz et al., 1997), indicating a methane production efficiency of 98.54 %. This correspondence indicates that daily methane output was equivalent to the expected methane yield from the daily PHBH feed (0.5 g VS/L-d), indicating a steady-state balance in methane production. Finally, after observing consistent methane production over an extended period in semi-batch mode, the reactor operation was terminated by halting the PHBH feed on day 99. The observed decreasing trend in methane production indicates the gradual depletion of methane precursors, with methane production ceasing completely by day 112 (Fig. 2A). Overall, the results presented here demonstrate that the AD process is an effective end-of-life treatment for PHBH-based products. It is worth mentioning that further studies are needed to evaluate reactor performance at higher OLRs. Also, future studies should focus on evaluating continuous anaerobic digesters operating on a mix of food waste or OFMSW and bioplastics, which entails a more realistic scenario for existing full-scale biogas plants.

3.2. *Characterization of degradation pattern of PHBH*

Visual inspection revealed that the bioplastic retained its structural sturdiness despite pronounced surface degradation, evidenced by the formation of pits and pores indicative of microbial activity, as confirmed by SEM analysis (Fig. 3A). Additionally, the XRD spectrum (Fig. 4A) demonstrated the preservation of the polymer's crystalline structure, with minimal variation in the intensity of characteristic diffraction peaks at 2θ values of 13.49°, 16.90°, 21.81°, 25.49°, 27.13°, and 30.31° (Farrag et al., 2022). The crystallinity index, calculated as the ratio of crystalline to amorphous peak areas within the 5–40° at 2θ range, remained relatively unchanged, further supporting the visual observation of structural sturdiness. The observed pattern of pore formation, combined with persistent crystallinity and a weight loss of approximately 52.85 ± 4.90 %, suggests that the degradation was likely driven by the non-uniform activity of extracellular microbial enzymes, which preferentially target susceptible regions (Bonartsev et al., 2012). In addition, the elemental mapping using EDAX coupled with SEM further confirmed a depletion of carbon-rich components within the eroded areas compared to the intact PHBH, providing additional evidence of

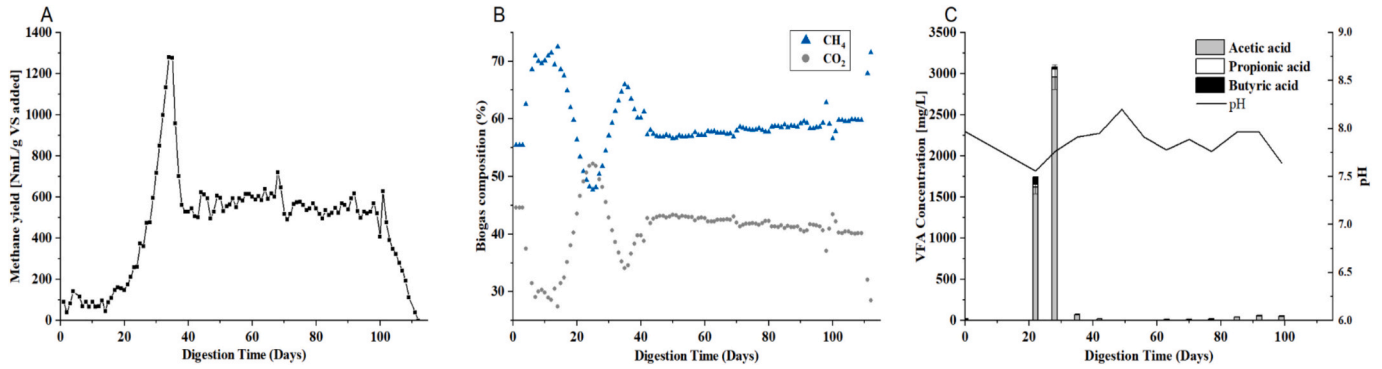

Fig. 2. Time course behaviour of (A) methane yield, (B) biogas composition, and (C) organic acids profile and pH during the semi-batch anaerobic digestion of PHBH.

degradation (Fig. 3B). These findings support the hypothesis of surface erosion, a degradation mechanism primarily attributed to the action of extracellular microbial enzymes. While both surface and bulk erosion can occur during polymer degradation, the limited diffusion of enzymes into the polymer matrix typically favours surface erosion in biological systems (Dotson et al., 2024).

Further, the FTIR-ATR analysis of the control and partially biodegraded material PHBH samples revealed several key spectral features indicative of chemical modifications that the polymeric structure underwent during its degradation (Fig. 4B). A broad peak at 3250–3650 cm^{-1}, corresponding to -OH stretching, was observed primarily in the control sample, with reduced intensity in the treated sample, suggesting polymer breakdown through hydrolysis. The presence of C—C and C—H stretching vibrations observed at 2935 cm^{-1} and 2860–3000 cm^{-1}, respectively, confirmed the aliphatic nature of the polymer backbone. This characteristic is attributed to the repeating aliphatic chains in the –[O–CH(CH_3)–CH_2–CO]– (3HB) and –[O–CH(CH_2(CH_2)$_3$$CH_3$)–$CH_2$–CO]– (3HH) units within the copolymer. The C—H stretching vibrations are attributed to the presence of the methyl (CH_3) and methylene (CH_2) groups present in both the shorter 3HB and the 3HH units. Notably, a reduction in the intensity of these peaks in the treated sample, indicates fragmentation of the long aliphatic chains, reflecting a change in the PHBH structure. A characteristic carbonyl (C=O) peak at 1700–1750 cm^{-1}, corresponding to the ester functional groups in the PHBH structure, was observed with varying intensities in both samples. The reduced intensity of this peak in the treated sample suggests a decrease in the number of intact ester linkages, indicating polymer degradation, further supporting polymer degradation (Coates, 2006; Nandiyanto et al., 2022). Unlike the 1500–4000 cm^{-1} region used for functional group identification, the fingerprint region (500–1500 cm^{-1}) contains complex, unique vibrational patterns specific to each compound, making it ideal for comparing treated and untreated samples (Coates, 2006; Nandiyanto et al., 2022). In this study, while both spectra exhibited similar peak patterns in the fingerprint region, the partially biodegraded material showed overall reduced peak intensities, indicating the breakdown of the polymeric structure of PHBH (Xu et al., 2019).

3.3. Microbial community analysis

The quality control (QC) metrics for the obtained sequence data of samples R1, R2, and R3 (see Supplementary material) highlight the reliability and accuracy of the sequencing results. All three samples consistently exhibited high-quality scores, with Q20 > 98 % and Q30 > 93 %, confirming the robustness of the sequencing data. During the pseudo-steady state of methane production, the microbial diversity within the anaerobic digester was evaluated through several alpha diversity metrics, including Chao1, Shannon Index, and Simpson indices. Both bacterial and archaeal communities exhibit a prokaryotic richness average of around 174 and 177, respectively, indicating the involvement of diverse microbiome in the system. The bacterial community showed richness values of 191, 193, and 140 for samples R1, R2, and R3, respectively, while the archaeal community exhibited richness values of 225, 133, and 173 for the same samples. This observed variation in species richness across the sample points reflects the distinct microbial community structures. The relatively lower richness observed in R3, particularly within the bacterial community, suggests a more specialized microbial profile. The periodic addition of PHBH likely promoted the establishment of a specialized microbial community optimized for the efficient degradation of PHBH, thereby promoting methane production (Bandini et al., 2022; Clagnan et al., 2023). Additionally, other metrics, such as the Shannon Index, which evaluates both species richness and evenness, yielded values of 4.801 for R1, 4.718 for R2, and 4.717 for R3 for the bacterial community, and 3.812 (R1), 2.42 (R2) and 3.02 (R3) for the archaeal community. These results indicate the presence of complex microbial ecosystems typical of AD systems (Zhang et al., 2021). The Simpson index, which evaluates species evenness and dominance, showed values of 0.919 for R1, 0.924 for R2, and 0.935 for R3 in the bacterial community, and 0.798 (R1), 0.543 (R2), and 0.637 (R3) for the archaeal community. The observed relatively similar Shannon index values and higher Simpson index values reflect a greater evenness in species distribution across all samples for bacteria. In the case of archaea, the lower Simpson index suggests a less even distribution and potentially higher dominance of certain archaeal species in the semi-batch reactor. These results highlight the stabilization of the microbial community within the anaerobic digester, indicating a well-established community.

A Principal Coordinate Analysis (PCoA) was conducted using Bray-Curtis, Jaccard Index, and Weighted UniFrac distances to evaluate the similarities and differences between samples. While the overall microbial community structure appeared broadly similar across the samples, minor variations were observed. The PCoA results, particularly with respect to Bray-Curtis distance and the Jaccard Index (Supplementary material), revealed a separation between the microbial communities of R1 and R3, with R2 occupying an intermediate position. This suggests that R2 may represent a transitional stage between R1 and R3, indicating a progression in microbial community composition over time. This observation was further supported by the alpha diversity analysis, which revealed significantly higher diversity in R1 and R2, with relatively lower diversity in R3. Regarding the archaeal communities, R2 and R3 exhibit greater similarity, while R1 comprises a slightly distinct community profile. This observed temporal shift in microbial community composition suggests an adaptive response to the continuous supply of PHBH (Clagnan et al., 2023).

As observed from alpha and beta diversity analysis, this pattern indicates a selective enrichment of microbial populations specialized in PHBH bioconversion to methane, highlighting the dynamic nature of microbial communities. This dynamic nature of microbial communities was effectively captured by performing UPGMA (Unweighted Pair

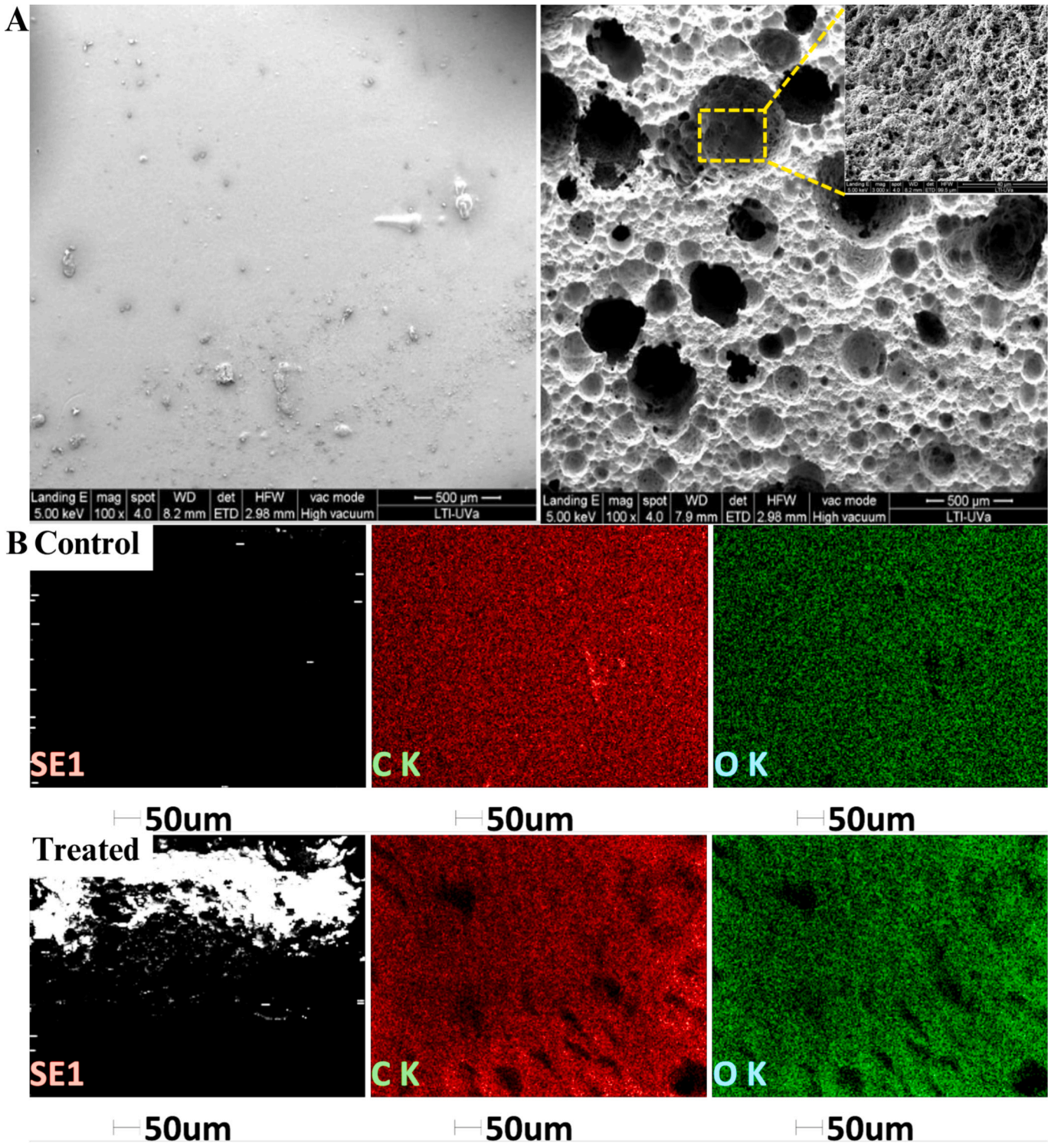

Fig. 3. (A) Morphological changes observed via Scanning Electron Microscopy (B) and elemental mapping by EDAX showing carbon depletion in eroded regions of PHBH in samples drawn on day 25.

Group Method with Arithmetic Mean) clustering based on Weighted UniFrac distance. The resulting dendrogram (Fig. 5) emphasizes the difference in the abundance of specific microbial groups as the semi-batch anaerobic digester evolved and stabilized.

Taxonomic analysis of the microbial communities during the pseudo-steady state revealed a diverse and complex ecosystem. *Firmicutes*, constituting 45.85 % (on average) of the total microbial population, emerged as the dominant phylum in this study. This observation is consistent with previous research that emphasizes the crucial role of *Firmicutes* in AD, particularly during the hydrolysis and acidogenesis stages (Yu et al., 2023). Members of this phylum are well-known for their ability to break down complex organic compounds into simpler molecules, thereby initiating the early phases of the digestion process (Le et al., 2024; Westerholm and Schnürer, 2019). The high abundance of *Firmicutes* in the digester indicates a strong hydrolytic potential, supporting the breakdown of organic matter and facilitating the

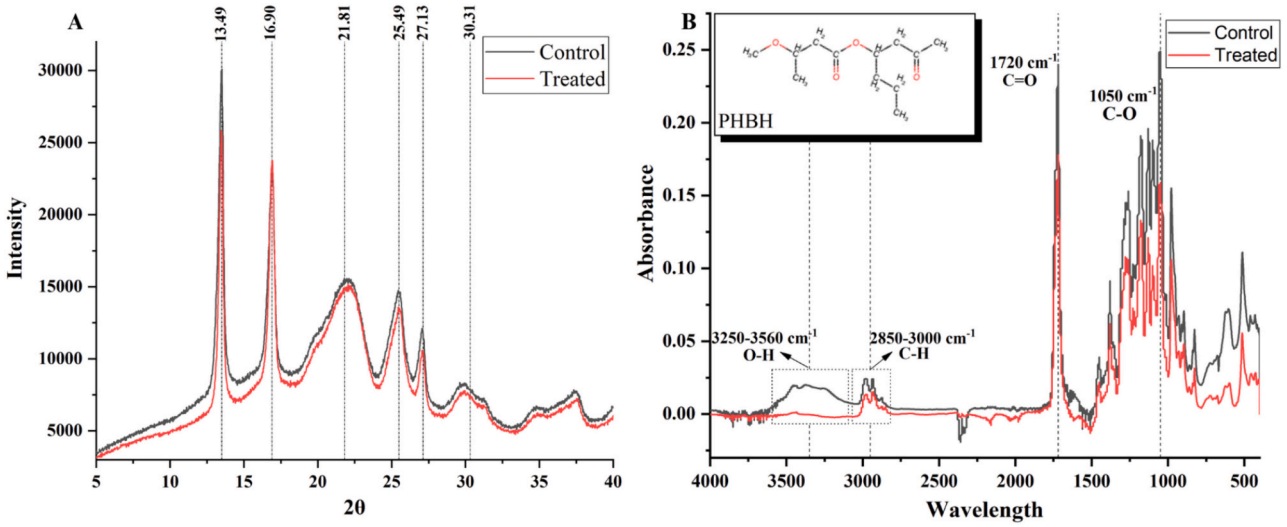

Fig. 4. Characterization of the partially degraded PHBH (A) XRD Spectra (B) FT-IR Spectra.

subsequent stages AD. The second most abundant phylum was *Cloacimonadota*, which accounted for an average of 18.03 % of the total community. *Cloacimonadota* has been reported as an understudied bacterial lineage frequently associated with engineered and wastewater systems (Johnson and Hug, 2022). On average, *Bacteroidota*, which is commonly associated with the fermentative processes in the acidogenic phase of AD (Braz et al., 2018; Loughrin et al., 2023), accounted for 12.6 % of the microbial population. Additionally, *Chloroflexi*, with an average relative abundance of 9.6 %, possesses hydrolase-coding genes that facilitate the breakdown of complex polymers into simpler monomers (Nierychlo et al., 2019). The role of *Synergistota*, which on average recorded a relative abundance of 6.4 %, in the anaerobic degradation of PHBH remains elusive. However, members of this phylum have been reported to be involved in syntrophic interactions with methanogens (Hardy et al., 2021; Tukanghan et al., 2021).

In contrast to the relatively stable bacterial community, the archaeal community exhibited notable variations across samples, indicating a dynamic archaeal structure with distinct phyla dominating at different stages of the system's progression. The most dominant archaeal phylum was *Halobacterota*, constituting an average of 67.26 % of the archaeal community. Its abundance increased significantly over time, from 49.90 % in R1 to 79.26 % in R2 and 72.63 % in R3. This upward trend suggests that *Halobacterota* plays a pivotal role in the methanization of PHBH. *Halobacterota* has been found in other anaerobic digesters systems (García-Depraect et al., 2024; Ottoni et al., 2022). *Euryarchaeota*, the second most prevalent phylum, accounted for an average of 11.62 % of the archaeal community. However, unlike *Halobacterota*, *Euryarchaeota* exhibited a decreasing trend, being more prominent in R1 (18.13 %) and R2 (13.25 %), with a marked decline in R3 (3.49 %). The observed decrease in our study may highlight the dominant role of *Halobacterota* as the system acclimates, leading to a relative reduction in *Euryarchaeota* (Fig. 5). Other archaeal phyla, such as *Thermoplasmatota* (2.14 %) and *Crenarchaeota* (0.41 %), were present in smaller proportions, suggesting their more limited role in the overall archaeal community.

At the genus level (Fig. 6A), *Anaerolineaceae*, representing 6.83 % of the bacterial population, was prominently identified, aligning with the observations of Jin et al. (2022) during the AD of poly(3-hydroxybutyrate-*co*-4-hydroxybutyrate). The role of *Anaerolineaceae* has been linked to the hydrolysis stage (Liang et al., 2016). Another significant genus identified was *Thermovirga*, representing 6.13 % of the bacterial community. Although less commonly linked to bioplastic degradation, its ability to ferment proteinaceous compounds and carbohydrates likely contributes to the metabolism of intermediate products generated during polymer breakdown, thus enhancing the efficiency of the AD process (Dahle and Birkeland, 2006).

The archaeal community was predominantly composed of acetoclastic methanogens, with *Methanosaeta* comprising 63.01 % (on average) of the archaeal population (Fig. 6B). This genus is crucial for the direct conversion of acetate to methane and carbon dioxide (Smith and Ingram-Smith, 2007), suggesting that the methanization of PHBH primarily occurred through acetoclastic methanogenesis. Other notable methanogenic genera included *Candidatus Methanofastidiosum* (9.49 %), *Methanoculleus* (3.65 %), *Methanobacterium* (1.88 %), and *Methanomassillicoccus* (1.85 %). These findings are consistent with the study by Liang et al. (2015), which identified *Anaerolineaceae* and *Methanosaeta* as dominant microbes in systems exposed to long-chain alkanes for extended periods, highlighting their critical roles in the degradation of complex polymers like PHBH (Liang et al., 2015). The observed co-dominance of *Anaerolineaceae* and *Thermovirga*, with the prevalence of *Methanosaeta* and other methanogens, suggests a well-adapted microbial community for effective PHBH degradation. In this system, *Anaerolineaceae*, along with other hydrolytic bacteria, likely initiates the breakdown of PHBH polymers, followed by *Thermovirga* and other genera involved in the breakdown of the resulting intermediates. *Methanosaeta*, supported by other methanogenic genera, converts these by-products into methane. It is worth noting that the microbiological results here observed provide valuable insights for the methanization of PHBH. However, future research integrating co-digestion (organic waste with bioplastics) with genome-centric metagenomic analysis could deepen our understanding of microbial roles, key enzymes, and their contributions to methane production during the AD of biodegradable bioplastics.

3.4. Digestate phytotoxicity testing

A concentration-dependent decrease in the germination index was observed with increasing digestate concentrations, resulting in complete inhibition at 20 % and 40 % concentrations, while 10 % digestate led to a drastic 70 % drop in the germination index compared to the control (Fig. 7A-B). The control set-up achieved a germination rate of approximately 84 %. Representative images of seeds showing complete and delayed germination are provided as supplementary material. Notably, some seeds at the 20 % digestate concentration exhibited delayed germination, characterized by minimal root growth (<1 mm). Despite visible signs of germination, these seeds were classified as ungerminated to ensure a consistent and unbiased evaluation of germination. This inhibitory effect observed on seed germination aligns with a recent study revealing the complex effects of bioplastics on soil and plant

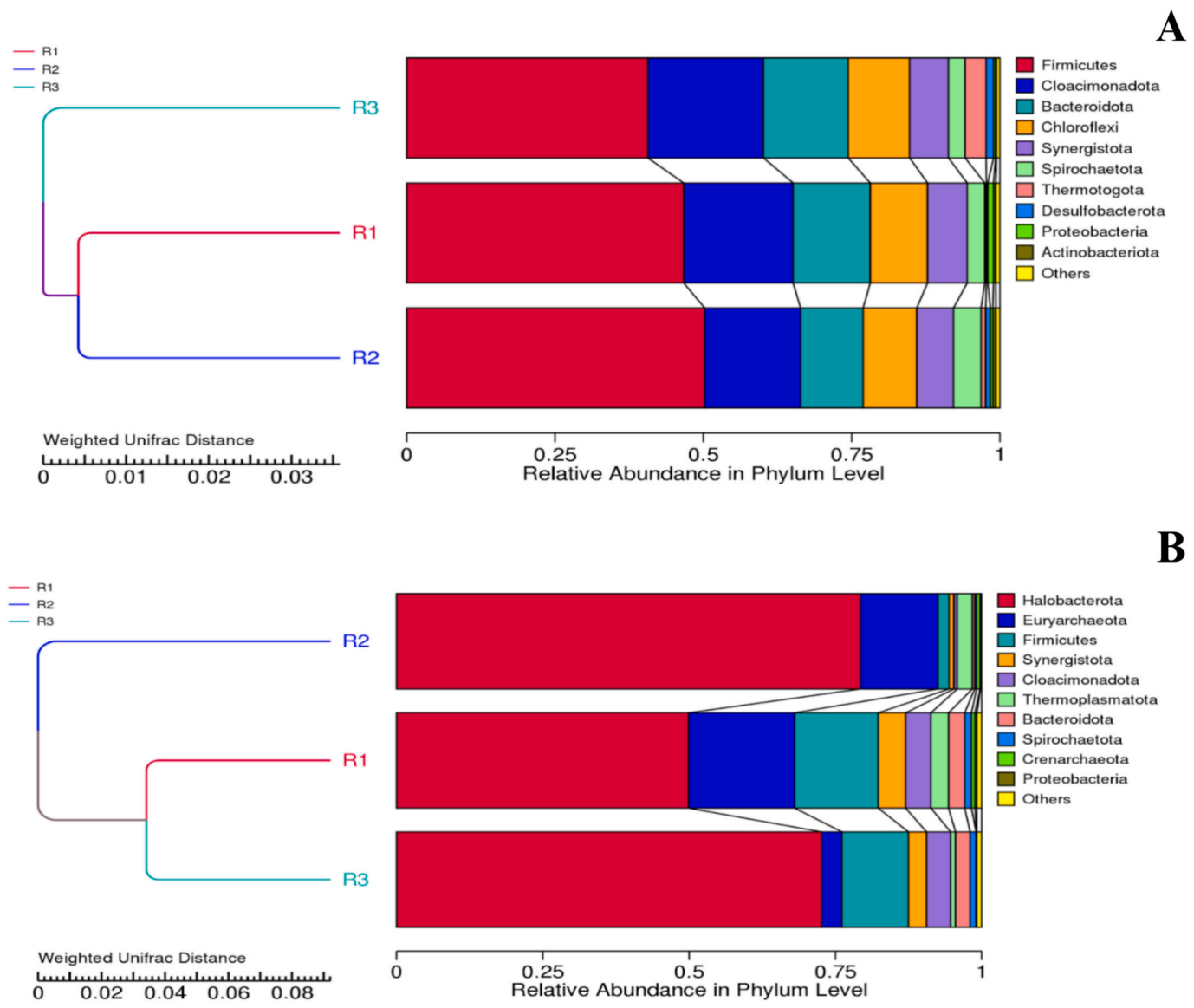

Fig. 5. Relative abundance of (A) bacterial and (B) archaeal communities at the phylum level during the semi-batch anaerobic digestion of PHBH under pseudo-steady-state conditions.

systems (Brown et al., 2023). PHBV bioplastics, when loaded onto soil at proportions exceeding 1 % of the total soil composition, significantly altered soil metabolomes and microbial communities, negatively affecting plant health and metabolic function (Brown et al., 2023). These findings suggest the presence of phytotoxic compounds within the digestate, likely VFAs and ammonia which could directly interfere with cellular processes essential for germination. These compounds might disrupt membrane integrity, enzyme activity, or hormonal signalling pathways critical for embryo activation and radicle emergence. Although VFA levels and total ammonia nitrogen levels (1.2 ± 0.2 g/L) were recorded to be below the inhibitory threshold for AD (Yang et al., 2024), these concentrations may have exerted phytotoxic effects on seed germination (Wang et al., 2022). Future investigation should identify specific inhibitory compounds within the digestate matrix and understand their interactions and impacts on plant growth. Despite these inhibitory effects, the byproducts of PHBH have been reported to indirectly benefit soil health. It has been reported that 3HB, a monomer of PHBH, has a positive effect on soil microbiota but a negative effect on plant growth by reducing nitrogen availability (Brtnicky et al., 2022). The phytotoxic effects observed in the digestate may pose risks for direct agricultural application and require careful management and further analysis to understand the inhibition mechanisms and develop mitigation strategies. Alternative strategies, such as co-digestion with food waste or nutrient-rich organic matter, could provide potentially beneficial results as a soil amendment. Expanding the study to include pot plant assays and germination tests will provide a more comprehensive understanding of the latent impact of digestates derived from the methanization of organic waste containing biodegradable bioplastics and their degradation by-products on plant growth and development.

4. Conclusions

This study provides a comprehensive analysis of the AD of PHBH under batch and semi-batch conditions. The batch system demonstrated the effective AD of PHBH, achieving a cumulative methane yield of 550.5 NmL CH_4/g VS added and a carbon recovery of 96.09 %, with 84.3 % converted to biogas. Structural analyses confirmed surface erosion as the primary biodegradation mechanism. In contrast, the semi-batch system with continuous feeding of PHBH allowed stable methane production, with an average yield of 562.34 NmL CH_4/g VS added and a

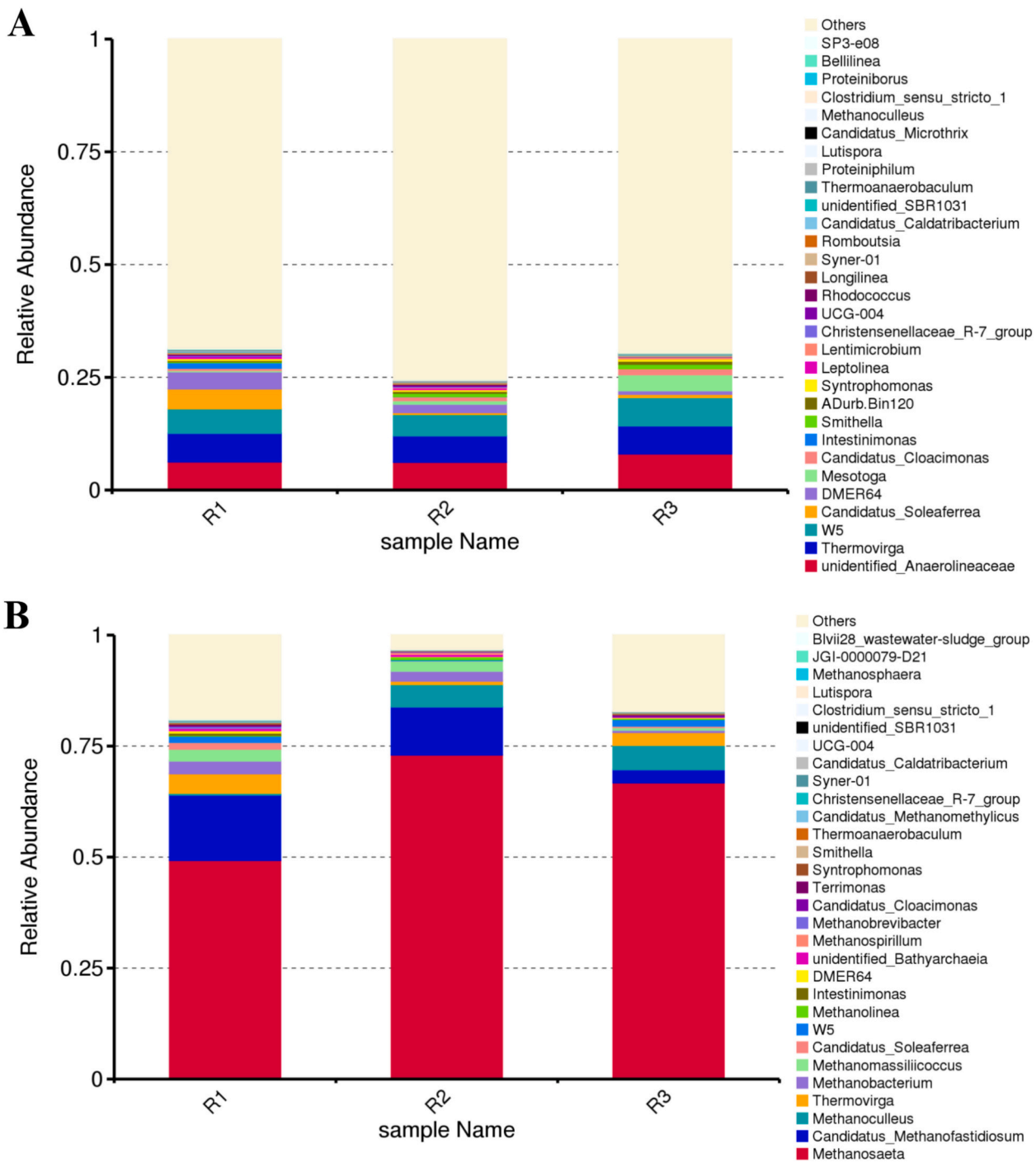

Fig. 6. Relative abundance of (A) bacterial and (B) archaeal communities at the genus level during the semi-batch digestion of PHBH under pseudo-steady-state conditions.

methene productivity of 281.17 NmL CH_4/L-d. The consistent substrate input supported microbial adaptation and ensured efficient degradation over extended periods. Microbial community analysis revealed that *Methanosaeta* dominated the archaeal population, suggesting aceto-clastic methanogenesis as the primary methane production pathway. However, digestate phytotoxicity tests indicated inhibitory effects on seed germination, emphasizing the need for further investigation into inhibitory compounds and mitigation strategies. Overall, operational strategies that enhance microbial adaptation and degradation should be prioritized for the efficient anaerobic degradation of biodegradable bioplastics such as PHBH. In particular, future research should focus on the implementation of continuous operation and co-digestion with complex bioplastic mixtures commonly found in urban biowaste.

CRediT authorship contribution statement

Mohamed Shafana Farveen: Writing – original draft, Visualization, Methodology, Investigation. **Raul Muñoz:** Writing – review & editing, Resources, Methodology. **Rajnish Narayanan:** Writing – review & editing, Supervision. **Octavio García-Depraect:** Writing – review & editing, Supervision, Resources, Project administration, Methodology, Formal analysis, Conceptualization.

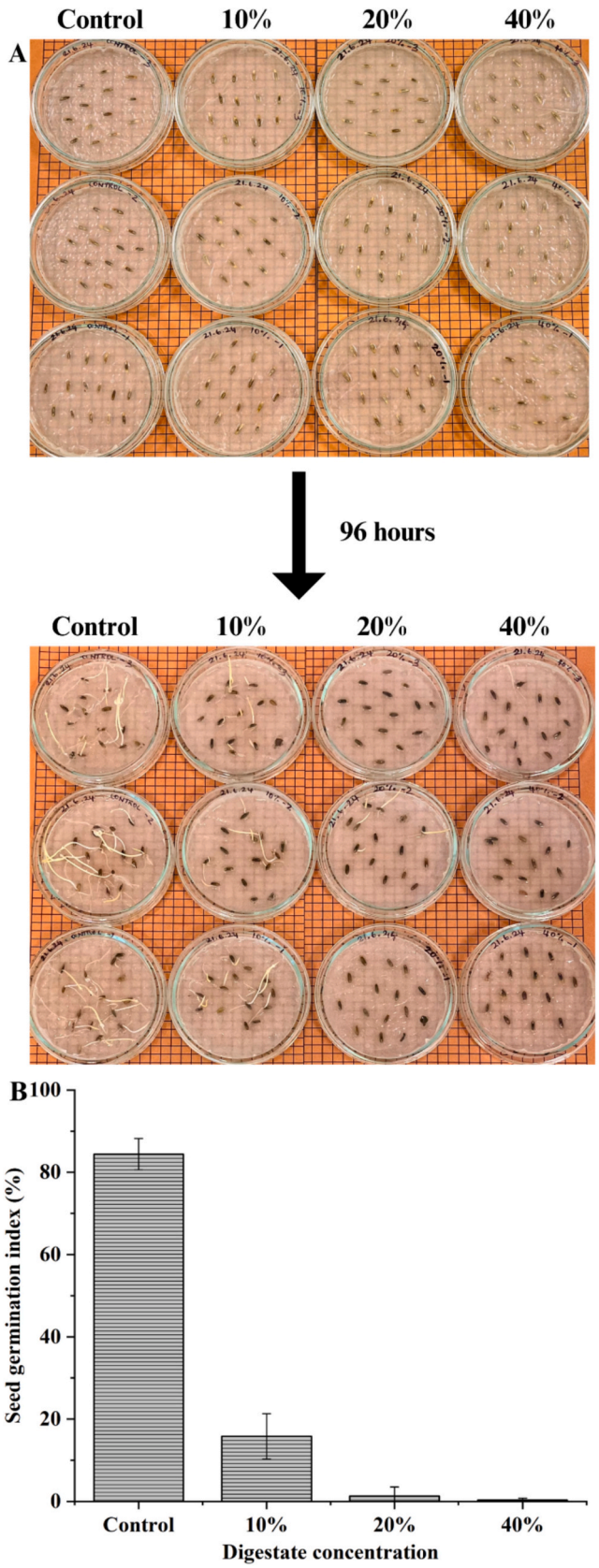

Fig. 7. Response of *Lolium perenne* seeds when exposed to digestate at varying concentration (A) Germination of *L. perenne* seeds (B) Seed germination index of *L. perenne* seeds.

Declaration of competing interest

The authors declare that they have no known competing financial interests or personal relationships that could have appeared to influence the work reported in this paper.

Acknowledgement

This work was supported by funding from the European Union's NextGeneration EU/PRTR and the MCIN/AEI/10.13039/501100011033 under Grant RYC2021-034559-I. We acknowledge the Erasmus+ KA171 program for supporting this research through a doctoral internship grant. We also acknowledge the support from the Regional Government of Castilla y León and the European FEDER Programme (CL-EI-2021–07 and UIC 379315). The authors gratefully acknowledge the invaluable technical support provided by Beatriz Estíbaliz Muñoz-González, Araceli Crespo-Rodríguez, Enrique José Marcos-Montero and Fernando González Pérez.

Appendix A. Supplementary data

Supplementary data to this article can be found online at https://doi.org/10.1016/j.scitotenv.2025.178794.

Data availability

Data will be made available on request.

References

Ahamed, A., Vallam, P., Iyer, N.S., Veksha, A., Bobacka, J., Lisak, G., 2021. Life cycle assessment of plastic grocery bags and their alternatives in cities with confined waste management structure: a Singapore case study. J. Clean. Prod. 278, 123956. https://doi.org/10.1016/j.jclepro.2020.123956.

American Public Health Association, 1995. Standard Methods for the Examination of Water and Wastewater, 19th edition.

Angelidaki, I., Alves, M., Bolzonella, D., Borzacconi, L., Campos, J.L., Guwy, A.J., Kalyuzhnyi, S., Jenicek, P., van Lier, J.B., 2009. Defining the biomethane potential (BMP) of solid organic wastes and energy crops: a proposed protocol for batch assays. Water Sci. Technol. 59, 927–934. https://doi.org/10.2166/wst.2009.040.

Atiwesh, G., Mikhael, A., Parrish, C.C., Banoub, J., Le, T.-A.T., 2021. Environmental impact of bioplastic use: a review. Heliyon 7, e07918. https://doi.org/10.1016/j.heliyon.2021.e07918.

Bandini, F., Vaccari, F., Soldano, M., Piccinini, S., Misci, C., Bellotti, G., Taskin, E., Cocconcelli, P.S., Puglisi, E., 2022. Rigid bioplastics shape the microbial communities involved in the treatment of the organic fraction of municipal solid waste. Front. Microbiol. 13, 1035561. https://doi.org/10.3389/fmicb.2022.1035561.

Bonartsev, A.P., Boskhomodgiev, A.P., Iordanskii, A.L., Bonartseva, G.A., Rebrov, A.V., Makhina, T.K., Myshkina, V.L., Yakovlev, S.A., Filatova, E.A., Ivanov, E.A., Bagrov, D.V., Zaikov, G.E., 2012. Hydrolytic degradation of poly(3-hydroxybutyrate), polylactide and their derivatives: kinetics, crystallinity, and surface morphology. Mol. Cryst. Liq. Cryst. 556, 288–300. https://doi.org/10.1080/15421406.2012.635982.

Braz, G.H.R., Fernandez-Gonzalez, N., Lema, J.M., Carballa, M., 2018. The time response of anaerobic digestion microbiome during an organic loading rate shock. Appl. Microbiol. Biotechnol. 102, 10285–10297. https://doi.org/10.1007/s00253-018-9383-9.

Brown, R.W., Chadwick, D.R., Zang, H., Graf, M., Liu, X., Wang, K., Greenfield, L.M., Jones, D.L., 2023. Bioplastic (PHBV) addition to soil alters microbial community structure and negatively affects plant-microbial metabolic functioning in maize. J. Hazard. Mater. 441, 129959. https://doi.org/10.1016/j.jhazmat.2022.129959.

Brtnicky, M., Pecina, V., Holatko, J., et al., 2022. Effect of biodegradable poly-3-hydroxybutyrate amendment on the soil biochemical properties and fertility under varying sand loads. Chem. Biol. Technol. Agric. 9, 75. https://doi.org/10.1186/s40538-022-00345-9.

Cazaudehore, G., Guyoneaud, R., Evon, P., Martin-Closas, L., Pelacho, A.M., Raynaud, C., Monlau, F., 2022. Can anaerobic digestion be a suitable end-of-life scenario for biodegradable plastics? A critical review of the current situation, hurdles, and challenges. Biotechnol. Adv. 56, 107916. https://doi.org/10.1016/j.biotechadv.2022.107916.

Cazaudehore, G., Guyoneaud, R., Lallement, A., Souquet, P., Gassie, C., Sambusiti, C., Grassl, B., Jiménez-Lamana, J., Cauzzi, P., Monlau, F., 2023a. Simulation of biowastes and biodegradable plastics co-digestion in semi-continuous reactors: performances and agronomic evaluation. Bioresour. Technol. 369, 128313. https://doi.org/10.1016/j.biortech.2022.128313.

Cazaudehore, G., Monlau, F., Gassie, C., Lallement, A., Guyoneaud, R., 2023b. Active microbial communities during biodegradation of biodegradable plastics by mesophilic and thermophilic anaerobic digestion. J. Hazard. Mater. 443, 130208. https://doi.org/10.1016/j.jhazmat.2022.130208.
Chernicharo, C.A., 2007. Biological Wastewater Treatment Series. IWA Publishing, London, England. doi:https://doi.org/10.2166/9781780402116.
Clagnan, E., Cucina, M., Vilas Sajgule, R., De Nisi, P., Adani, F., 2023. Microbial community acclimatization enhances bioplastics biodegradation and biogas production under thermophilic anaerobic digestion. Bioresour. Technol. 390, 129889. https://doi.org/10.1016/j.biortech.2023.129889.
Coates, J., 2006. Interpretation of infrared spectra, a practical approach. In: Encyclopedia of Analytical Chemistry. https://doi.org/10.1002/9780470027318.A5606.
Cucina, M., De Nisi, P., Trombino, L., Tambone, F., Adani, F., 2021. Degradation of bioplastics in organic waste by mesophilic anaerobic digestion, composting and soil incubation. Waste Manag. 134, 67–77. https://doi.org/10.1016/j.wasman.2021.08.016.
Dahle, H., Birkeland, N.-K., 2006. *Thermovirga lienii* gen. nov., sp. nov., a novel moderately thermophilic, anaerobic, amino-acid-degrading bacterium isolated from a North Sea oil well. Int. J. Syst. Evol. Microbiol. 56, 1539–1545. https://doi.org/10.1099/ijs.0.63894-0.
Dolci, G., Venturelli, V., Catenacci, A., Ciapponi, R., Malpei, F., Romano Turri, S.E., Grosso, M., 2022. Evaluation of the anaerobic degradation of food waste collection bags made of paper or bioplastic. J. Environ. Manag. 305, 114331. https://doi.org/10.1016/j.jenvman.2021.114331.
Dotson, K.W., Pisano, K., Renegar, D.A., 2024. Surface erosion equations for degradation analysis of several common three-dimensional shapes of plastic materials. J. Polym. Environ. https://doi.org/10.1007/s10924-024-03291-9.
Edgar, R.C., 2004. MUSCLE: a multiple sequence alignment method with reduced time and space complexity. BMC Bioinformatics 5, 113. https://doi.org/10.1186/1471-2105-5-113.
Edgar, R.C., Haas, B.J., Clemente, J.C., Quince, C., Knight, R., 2011. UCHIME improves sensitivity and speed of chimera detection. Bioinformatics 27, 2194–2200. https://doi.org/10.1093/bioinformatics/btr381.
Eraslan, K., Aversa, C., Nofar, M., Barletta, M., Gisario, A., Salehiyan, R., Goksu, Y.A., 2022. Poly(3-hydroxybutyrate-co-3-hydroxyhexanoate) (PHBH): synthesis, properties, and applications - a review. Eur. Polym. J. 167, 111044. https://doi.org/10.1016/j.eurpolymj.2022.111044.
Farrag, Y., Barral, L., Gualillo, O., Moncada, D., Montero, B., Rico, M., Bouza, R., 2022. Effect of different plasticizers on thermal, crystalline, and permeability properties of poly(3-hydroxybutyrate-co-3-hydroxyhexanoate) films. Polymers 14, 3503. https://doi.org/10.3390/polym14173503.
Ganguly, R.K., Chakraborty, S.K., 2024. Plastic waste management during and post Covid19 pandemic: challenges and strategies towards circular economy. Heliyon 10, e25613. https://doi.org/10.1016/j.heliyon.2024.e25613.
García-Depraect, O., Lebrero, R., Rodriguez-Vega, S., Bordel, S., Santos-Beneit, F., Martínez-Mendoza, L.J., Aragão Börner, R., Börner, T., Muñoz, R., 2022a. Biodegradation of bioplastics under aerobic and anaerobic aqueous conditions: kinetics, carbon fate and particle size effect. Bioresour. Technol. 344, 126265. https://doi.org/10.1016/j.biortech.2021.126265.
García-Depraect, O., Lebrero, R., Rodriguez-Vega, S., Börner, R.A., Börner, T., Muñoz, R., 2022b. Production of volatile fatty acids (VFAs) from five commercial bioplastics via acidogenic fermentation. Bioresour. Technol. 360, 127655. https://doi.org/10.1016/j.biortech.2022.127655.
García-Depraect, O., Lebrero, R., Martínez-Mendoza, L.J., Rodriguez-Vega, S., Aragão Börner, R., Börner, T., Muñoz, R., 2023. Enhancement of biogas production rate from bioplastics by alkaline pretreatment. Waste Manag. 164, 154–161. https://doi.org/10.1016/j.wasman.2023.04.009.
García-Depraect, O., Martínez-Mendoza, L.J., Aragão Börner, R., Zimmer, J., Muñoz, R., 2024. Biomethanization of rigid packaging made entirely of poly(3-hydroxybutyrate-co-3-hydroxyhexanoate): mono- and co-digestion tests and microbial insights. Bioresour. Technol. 408, 131180. https://doi.org/10.1016/j.biortech.2024.131180.
Hardy, J., Bonin, P., Lazuka, A., Gonidec, E., Guasco, S., Valette, C., Lacroix, S., Cabrol, L., 2021. Similar methanogenic shift but divergent syntrophic partners in anaerobic digesters exposed to direct versus successive ammonium additions. Microbiol. Spectr. 9, e0080521. https://doi.org/10.1128/Spectrum.00805-21.
Himanshu, H., Voelklein, M.A., Murphy, J.D., Grant, J., O'Kiely, P., 2017. Factors controlling headspace pressure in a manual manometric BMP method can be used to produce a methane output comparable to AMPTS. Bioresour. Technol. 238, 633–642. https://doi.org/10.1016/j.biortech.2017.04.088.
Jin, Y., Cai, F., Song, C., Liu, G., Chen, C., 2022. Degradation of biodegradable plastics by anaerobic digestion: morphological, micro-structural changes and microbial community dynamics. Sci. Total Environ. 834, 155167. https://doi.org/10.1016/j.scitotenv.2022.155167.
Johnson, L.A., Hug, L.A., 2022. Cloacimonadota metabolisms include adaptations in engineered environments that are reflected in the evolutionary history of the phylum. Environ. Microbiol. Rep. 14, 520–529. https://doi.org/10.1111/1758-2229.13061.
Koch, K., Hafner, S.D., Weinrich, S., Astals, S., Holliger, C., 2020. Power and limitations of biochemical methane potential (BMP) tests. Front. Energy Res. 8. https://doi.org/10.3389/fenrg.2020.00063.
Le, T.-S., Bui, X.-T., Nguyen, P.-D., Hao Ngo, H., Dang, B.-T., Le Quang, D.-T., Thi Pham, T., Visvanathan, C., Diels, L., 2024. Bacterial community composition in a two-stage anaerobic membrane bioreactor for co-digestion of food waste and food court wastewater. Bioresour. Technol. 391, 129925. https://doi.org/10.1016/j.biortech.2023.129925.
Liang, B., Wang, L.-Y., Mbadinga, S.M., Liu, J.-F., Yang, S.-Z., Gu, J.-D., Mu, B.-Z., 2015. Anaerolineaceae and Methanosaeta turned to be the dominant microorganisms in alkanes-dependent methanogenic culture after long-term of incubation. AMB Express 5, 117. https://doi.org/10.1186/s13568-015-0117-4.
Liang, B., Wang, L.-Y., Zhou, Z., Mbadinga, S.M., Zhou, L., Liu, J.-F., Yang, S.-Z., Gu, J.-D., Mu, B.-Z., 2016. High frequency of Thermodesulfovibrio spp. and anaerolineaceae in association with Methanoculleus spp. in a long-term incubation of n-alkanes-degrading methanogenic enrichment culture. Front. Microbiol. 7, 1431. https://doi.org/10.3389/fmicb.2016.01431.
Loughrin, J.H., Parekh, R.R., Agga, G.E., Silva, P.J., Sistani, K.R., 2023. Microbiome diversity of anaerobic digesters is enhanced by microaeration and low frequency sound. Microorganisms 11. https://doi.org/10.3390/microorganisms11092349.
Magoč, T., Salzberg, S.L., 2011. FLASH: fast length adjustment of short reads to improve genome assemblies. Bioinformatics 27, 2957–2963. https://doi.org/10.1093/bioinformatics/btr507.
Martínez-Cruz, A., Rojas-Valencia, M.N., 2024. Assessment of phytotoxicity in untreated and electrochemically treated leachates through the analysis of early seed growth and inductively coupled plasma-optical emission spectroscopy characterization. Horticulturae 10, 67. https://doi.org/10.3390/horticulturae10010067.
Nandiyanto, A.B.D., Ragadhita, R., Fiandini, M., 2022. Interpretation of Fourier transform infrared spectra (FTIR): a practical approach in the polymer/plastic thermal decomposition. Indones. J. Sci. Technol. 8, 113–126. https://doi.org/10.17509/ijost.v8i1.53297.
Nierychlo, M., Milobedzka, A., Petriglieri, F., McIlroy, B., Nielsen, P.H., McIlroy, S.J., 2019. The morphology and metabolic potential of the Chloroflexi in full-scale activated sludge wastewater treatment plants. FEMS Microbiol. Ecol. 95. https://doi.org/10.1093/femsec/fiy228.
Ottoni, J.R., Bernal, S.P.F., Marteres, T.J., Luiz, F.N., Dos Santos, V.P., Mari, Â.G., Somer, J.G., de Oliveira, V.M., Passarini, M.R.Z., 2022. Cultured and uncultured microbial community associated with biogas production in anaerobic digestion processes. Arch. Microbiol. 204, 340. https://doi.org/10.1007/s00203-022-02819-8.
Quast, C., Pruesse, E., Yilmaz, P., Gerken, J., Schweer, T., Yarza, P., Peplies, J., Glöckner, F.O., 2013. The SILVA ribosomal RNA gene database project: improved data processing and web-based tools. Nucleic Acids Res. 41, D590–D596. https://doi.org/10.1093/nar/gks1219.
Raposo, F., Fernández-Cegrí, V., De la Rubia, M.A., Borja, R., Béline, F., Cavinato, C., Demirer, G., Fernández, B., Fernández-Polanco, M., Frigon, J.C., Ganesh, R., Kaparaju, P., Koubova, J., Méndez, R., Menin, G., Peene, A., Scherer, P., Torrijos, M., Uellendahl, H., Wierinck, I., de Wilde, V., 2011. Biochemical methane potential (BMP) of solid organic substrates: evaluation of anaerobic biodegradability using data from an international interlaboratory study. J. Chem. Technol. Biotechnol. 86, 1088–1098. https://doi.org/10.1002/jctb.2622.
Reischwitz, A., Stoppok, E., Buchholz, K., 1997. Anaerobic degradation of poly-3-hydroxybutyrate and poly-3-hydroxybutyrate-co-3-hydroxyvalerate. Biodegradation 8, 313–319. https://doi.org/10.1023/a:1008203525476.
Ryan, C.A., Billington, S.L., Criddle, C.S., 2017. Assessment of models for anaerobic biodegradation of a model bioplastic: poly(hydroxybutyrate-co-hydroxyvalerate). Bioresour. Technol. 227, 205–213. https://doi.org/10.1016/j.biortech.2016.11.119.
Selvaranjan, K., Navaratnam, S., Rajeev, P., Ravintherakumaran, N., 2021. Environmental challenges induced by extensive use of face masks during COVID-19: a review and potential solutions. Environmental Challenges 3, 100039. https://doi.org/10.1016/j.envc.2021.100039.
Shrestha, A., van-Eerten Jansen, M.C.A.A., Acharya, B., 2020. Biodegradation of bioplastic using anaerobic digestion at retention time as per industrial biogas plant and international norms. Sustain. Sci. Pract. Policy 12, 4231. https://doi.org/10.3390/su12104231.
Slepetiene, A., Volungevicius, J., Jurgutis, L., Liaudanskiene, I., Amaleviciute-Volunge, K., Slepetys, J., Ceseviciene, J., 2020. The potential of digestate as a biofertilizer in eroded soils of Lithuania. Waste Manag. 102, 441–451. https://doi.org/10.1016/j.wasman.2019.11.008.
Smith, K.S., Ingram-Smith, C., 2007. Methanosaeta, the forgotten methanogen? Trends Microbiol. 15, 150–155. https://doi.org/10.1016/j.tim.2007.02.002.
Tukanghan, W., Hupfauf, S., Gómez-Brandón, M., Insam, H., Salvenmoser, W., Prasertsan, P., Cheirsilp, B., O-Thong, S., 2021. Symbiotic Bacteroides and Clostridium-rich methanogenic consortium enhanced biogas production of high-solid anaerobic digestion systems. Bioresource Technology Reports 14, 100685. https://doi.org/10.1016/j.biteb.2021.100685.
Wang, G., Yang, Y., Kong, Y., Ma, R., Yuan, J., Li, G., 2022. Key factors affecting seed germination in phytotoxicity tests during sheep manure composting with carbon additives. J. Hazard. Mater. 421, 126809. https://doi.org/10.1016/j.jhazmat.2021.126809.
Westerholm, M., Schnürer, A., 2019. Microbial responses to different operating practices for biogas production systems. In: Rajesh Banu, J. (Ed.), Anaerobic Digestion. https://doi.org/10.5772/intechopen.73348. IntechOpen.
Xu, H.-S., Zhu, L., Mei, Y., 2021. Effects of high levels of nitrogen and phosphorus on perennial ryegrass (*Lolium perenne L.*) and its potential in bioremediation of highly eutrophic water. Environ. Sci. Pollut. Res. Int. 28, 9475–9483. https://doi.org/10.1007/s11356-020-11458-9.
Xu, X., Li, J., Ma, L., Ma, X., 2019. Preparation and properties of biocomposite from poly (3-hydroxybutyrate-co-3-hydroxyhexanoate) reinforced with regenerated cellulose. Cellulose 26, 5427–5436. https://doi.org/10.1007/s10570-019-02460-7.

Yan, X., Zhou, W., Ma, X., Sun, B., 2021. Fabrication and characterization of poly(3-hydroxybutyrate-co-3-hydroxyhexanoate) modified with nano-montmorillonite biocomposite. E-polymers 21, 038–046. https://doi.org/10.1515/epoly-2021-0006.

Yang, J., Zhang, J., Du, X., Gao, T., Cheng, Z., Fu, W., Wang, S., 2024. Ammonia inhibition in anaerobic digestion of organic waste: a review. Int. J. Environ. Sci. Technol. (Tehran). https://doi.org/10.1007/s13762-024-06029-1.

Yu, C., Dongsu, B., Tao, Z., Xintong, J., Ming, C., Siqi, W., Zheng, S., Yalei, Z., 2023. Anaerobic co-digestion of three commercial bio-plastic bags with food waste: effects on methane production and microbial community structure. Sci. Total Environ. 859, 159967. https://doi.org/10.1016/j.scitotenv.2022.159967.

Zhang, L., Gong, X., Wang, L., Guo, K., Cao, S., Zhou, Y., 2021. Metagenomic insights into the effect of thermal hydrolysis pre-treatment on microbial community of an anaerobic digestion system. Sci. Total Environ. 791, 148096. https://doi.org/10.1016/j.scitotenv.2021.148096.

Zhang, M., Gao, B., Chen, J., Li, Y., 2015. Effects of graphene on seed germination and seedling growth. J. Nanopart. Res. 17. https://doi.org/10.1007/s11051-015-2885-9.

Zhu, X., Zhu, S., Zhao, Z., Kang, X., Ju, F., 2023. Microbiome dynamics during anaerobic digestion of food waste and the genetic potential for poly (lactic acid) co-digestion. Chem. Eng. J. 473, 145194. https://doi.org/10.1016/j.cej.2023.145194.